eTransportation 23 (2025) 100389

Contents lists available at ScienceDirect

eTransportation

journal homepage: www.journals.elsevier.com/etransportation

Business cases for degradation-aware bidirectional charging of residential users and heavy-duty vehicle fleets

David Menchaca Santos, Pauline Thüne, Jan Martin Zepter *, Mattia Marinelli

Department of Wind and Energy Systems, Technical University of Denmark (DTU), Frederiksborgvej 399, 4000 Roskilde, Denmark

ARTICLE INFO

Keywords:
Battery degradation
Electric heavy-duty fleet
Electric vehicles
Frequency disturbance
Price arbitrage
Vehicle-to-X

ABSTRACT

In the push towards decarbonizing the transport sector, integrating electric vehicles (EVs) is crucial. Vehicle-to-everything services can address concerns about EV acceptance and grid integration, but viable business models are necessary to incentivize user participation. This paper presents a techno-economic mixed integer linear programming optimization model to assess the feasibility of bidirectional charging for residential users (RUs) and heavy-duty fleet vehicles. The model ensures proper battery degradation management and integrates renewable energy sources at charging locations. Price arbitrage (PA), specifically vehicle-to-home (V2H) and residential vehicle-to-grid (V2G), is explored for RUs. For larger EV fleets, V2G PA and V2G combined with frequency containment reserve for disturbances (FCR-D) are investigated. Business cases guide the optimization, simulating a year of operation in Eastern Denmark. The results are compared to a baseline scenario with no bidirectional charging capability. RUs achieve average cost savings of 176 € with a payback period of 5 to 23 years, depending on the charging equipment supplier. V2H proves most suitable for *remote* users with flexible charging patterns. While EV fleets do not see significant savings with V2G alone, V2G combined with FCR-D yields savings of 330 thousand € with a payback period of 3 to 17 years. Challenges remain due to the rarity of commercially available bidirectional charging equipment and limited data on driving patterns. However, our analysis shows that bidirectional charging offers substantial financial incentives for both RUs and fleet managers, promoting EV adoption and advancing transport sector decarbonization.

1. Introduction

Due to their rapid development, inherently high efficiency, and lowering costs, electric vehicles (EVs) have become the key technology to decarbonize the road transport sector which accounts for over 22% of Europe's total net emissions in 2022 [1]. EVs' improved range, wider model availability and increased performance have boosted their attractiveness to consumers [2], and consequently led to their exponential growth in sales [3]. In fact, the International Energy Agency (IEA) considers EVs to be one of the few clean energy components of the energy system that are on track to achieve net zero CO_2 emissions by mid-century [4]. However, rapid and massive growth of electric vehicles can present several challenges, such as grid congestion, increased EV charging with non-renewable energy, and accelerated battery degradation [5,6]. These challenges can be faced by vehicle-to-everything (V2X) services, enabling the coordination with renewable energy sources (RESs) to align flexible consumption with grid needs [7] and deriving extra value from the battery assets during times when EVs are not used for driving [8,9]. Then, V2X becomes of crucial importance for the mass deployment of EVs.

One common classification by Thompson et al. [8] divides V2X services according to the infrastructure they serve, sorting them into vehicle-to-home (V2H), vehicle-to-building (V2B), and vehicle-to-grid (V2G). V2H focuses exclusively on optimizing household electricity consumption with an EV, which may also act as a backup power source. Vehicle-to-building (V2B) serves the same purpose for commercial and industrial buildings using aggregated EV fleets. Finally, V2G describes all energy or power services provided to the grid via an EV battery. Here, a modification suggested by [10] reserves V2G for services targeting grid operators. However, the boundaries between these classifications remain vague, as two services may be addressed simultaneously, such as V2H and V2G in the form of peak shaving through energy arbitrage operations. In such cases, the largest involved infrastructure of the service is considered for the naming in this paper.

Bidirectional charging and discharging facilitate the concept of V2X, even more so with their increasing readiness. They allow EV owners to provide electricity to the grid or offer ancillary services. Adjusting the charging and discharging profiles of EVs can assist in enabling the advantages of V2X [9]. For instance, V2X reduces ownership cost of

* Corresponding author.
E-mail address: jmwze@dtu.dk (J.M. Zepter).

https://doi.org/10.1016/j.etran.2024.100389
Received 30 July 2024; Received in revised form 1 November 2024; Accepted 28 December 2024
Available online 3 January 2025

EVs, provides backup storage, solves issues associated with renewable energy and grid congestion, balances the grid, among others; all of this potentially reducing electricity costs. However, to do so, stakeholders need to be able to manage the charging and discharging of EVs, as well as benefit from exploiting their assets for a service separate from the primary function of mobility. Therefore, numerous research efforts deal with the development of operational models and algorithms for V2X implementation and their demonstration in pilot projects [10]. A detailed overview of the state-of-the-art in V2X research is presented in Section 2.1, though most studies prioritize the perspective of grid planners, charge point operators, or EV aggregators. Since V2X concepts are still in early development, particularly with the upcoming readiness of bidirectional charging, it is crucial to analyze associated business models and assess their feasibility based on both technical capabilities of the equipment as well as economic factors for the end-users involved. A key factor influencing the viability of these business models is battery degradation because EV users ought to be fairly compensated for their participation in V2X services. Evaluating and demonstrating the viability of business models that effectively consider battery degradation can encourage user engagement in V2X and exploit the system benefits of the mass deployment of EVs.

1.1. Scientific contributions

The goal of this paper is to assess the feasibility of bidirectional charging in light of appropriate battery degradation considerations. We apply our derived methodology to real-life case studies in Eastern Denmark (DK2). The scientific contributions can be summarized as follows:

- This study provides a selection and design of profitable business models for bidirectional charging.
- As opposed to many works in existing literature, this study quantifies the benefits of V2X specifically from the perspective of households and heavy-duty EV fleets.
- This study proposes a new method to determine the costs associated with calendar and cycle degradation independently. Specifically, it models calendar degradation with base and additional degradation factors that depend on a state of charge (SOC) threshold. Additionally, it includes seasonal variations to account for the effects of ambient temperatures on calendar degradation.

The paper aims to identify feasible V2X services that reduce the cost of ownership of EVs for end-users, assessing their profitability and operational costs.

1.2. Paper outline

The remainder of the paper is structured as follows: Section 2 reviews the state-of-the-art on V2X research and details the selection of V2X services aligned with the developed business models. Section 3 describes the battery degradation costs and the techno-economic mixed-integer linear optimization implemented to simulate bidirectional V2X operation. Section 4 presents the case study and selected data to contextualize the V2X models within a real-life setting. Lastly, Section 5 analyses and discusses the modeling results, while Section 6 concludes the work.

2. Literature review and business model selection

This section reviews the related work on optimal scheduling of EVs with bidirectional charging capability analyzing cost and profitability of V2X while considering models of calendar and cycle battery degradation. The literature highlights the users and services for which business models are selected and developed. Finally, the four selected business models are described.

2.1. State-of-the-art V2X research

In the context of V2X, cost savings are generally achieved through electricity price differences by charging EVs during hours of low prices and/or discharging at times of high prices, formally known as price arbitrage (PA). Other revenue streams include active/reactive power support, congestion mitigation, harmonic compensation, peak shaving, RES integration, as well as voltage and frequency regulation [9,11]. The latter involves a control mechanism within power systems that activates reserves in response to frequency deviations. A detailed overview of operational strategies in the context of V2X is provided in [9].

Among V2X services with bidirectional capability, V2G is to date the most researched. Gough et al. [12] conclude that net income generation in V2G is strongly dependent upon associated cycle battery degradation costs. When accounting for these costs, participating in capacity market and wholesale market trading yields the highest income for an EV parking lot associated with a commercial building. Other V2G services do not generate sufficient income. Lotfi et al. [13] show that EVs can support the electric grid of a smart city while reducing costs for EV owners. Similarly, Wu and Lin [14] prove V2G technology can significantly enhance the power grid load factor and reduce power supply costs, but it requires an effective business model to transfer these benefits to EV owners and encourage adoption. Additionally, Ahmadian et al. [15] state V2G offers greater benefits over smart charging to EV owners, though these are offset by battery degradation costs due to increased energy throughput. Geng et al. [16] proved that strategies that minimize battery degradation in V2G services, frequency regulation and peak shaving, yield the highest net profits by avoiding premature battery replacement, while Leippi et al. [17] warn EV owners could make a loss if battery degradation is not compensated in a V2G enabled PA scheme within an industrial smart grid. In essence, the implementation of V2G services, like PA and reserve provision, benefits its stakeholders as long as EV users get compensated for their battery degradation.

Among these users, EV fleets recently gained increased attention in literature. Latest research [18–20] highlights the potential of public electric bus fleets in providing regulation services and participating in energy trading. On top, several pilot projects launched trials for investigating EV fleets offering PA or transmission system operator (TSO) services [21,22], with technical feasibility proven, as stated by [10,23]. Some examples of the most recent trials include electric bus fleets like Bus2Grid [24,25], Blue Bird School Bus V2G commercialization project [26], and V2Go [27,28]. On the contrary, only a few studies examine the participation of general EV users providing grid services in the market. Notably, Zheng et al. [29] optimized the potential profits of EVs with home-based or workplace-based charging. Their findings indicate that the generated revenue alone could not cover the incurred degradation cost.

One aspect needing further attention is the incorporation of relevant stress factors on battery degradation into cost optimization models, which remains of limited investigation [6]. In general, battery degradation models can be categorized into electrochemical, data-driven, and semi-empirical models. The most comprehensive battery degradation models for optimizing cost savings in the literature are, to the best of our knowledge, the following. Ahmadian et al. [15] minimized the operational and degradation costs of EVs by modeling calendar and cycle degradation based on experimental data. Calendar degradation was represented as an exponential function of SOC, ambient temperature, and time, while cycle degradation was modeled as a function of depth of discharge and C-rate. Similarly, Recalde et al. [30] also accounted for cycle degradation using depth of discharge and C-rate in a robust scheduling mechanism for an interruptible load aggregator, addressing uncertainties in energy and reserve prices. Lyu et al. [31] proposed a semi-empirical battery cycle wear model based on depth of discharge and accumulated charge cycles to optimize an aggregator's income from PA and the provision of regulation services. Khezri et al. [32]

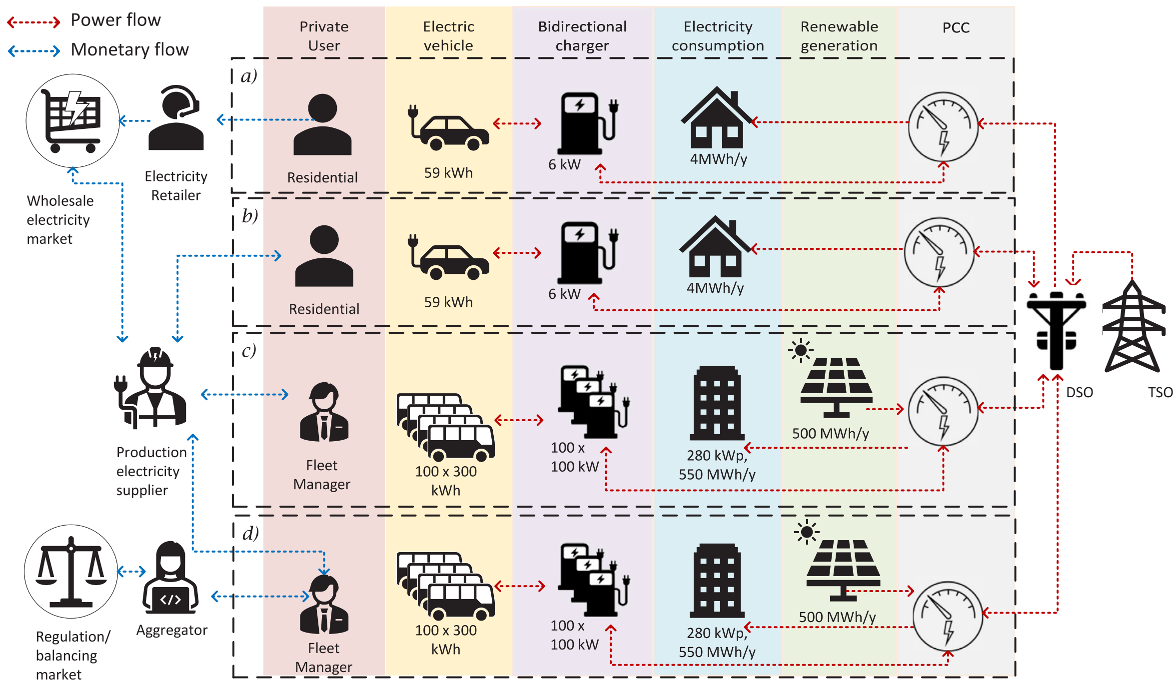

Fig. 1. Agents and assets of the investigated business models: (a) V2H, (b) Residential V2G, (c) Fleet V2G, (d) Fleet V2G + FCR-D.

introduced a detailed semi-empirical piece-wise linear approximation for calendar and cycle aging in a mixed integer linear programming (MILP) model aimed at minimizing EV charging and discharging costs. Their model results show that SOC and energy throughput are key factors to consider for the degradation process. Furthermore, Montes et al. [6] conclude that models considering SOC achieve greater cost reductions than those focusing on charge-discharge rate (C-rate). In line with this, Wikner and Thiringer [33] state that minimizing periods at high SOC is the most effective battery preserving strategy. The authors in [6] advocate for semi-empirical models due to their reduced data requirements and shorter execution times. They propose a semi-empirical model which utilizes SOC degradation cost tables that relate to battery conditions, and also separates between cycle and calendar degradation for a unidirectional charging optimization. Remarkably, to effectively sustain battery lifetime due to increased usage under V2G operation, battery degradation modeling must prioritize SOC and energy throughput.

In summary, the existing literature reveals a gap in optimization efforts aimed primarily at minimizing the ownership cost of EVs. Greater emphasis should be placed on EV users, as their willingness to participate in V2X services largely depends on how effectively battery degradation is addressed. Hence, it is important to analyze business models for the common residential EV user but also for emerging EV fleets; for instance those enabled by bidirectional charging: PA and reserve services. Furthermore, only a limited number of V2X research considers battery degradation models that account for both calendar and cycle effects on battery aging. Notably, significant potential exists for extending battery lifetime by avoiding high SOC values and optimizing the increased energy throughput of an EV battery under V2G operation. Finally, most of the reviewed literature on operational strategies focuses on light-duty EVs, disregarding the potential benefits for heavy-duty EV fleets.

2.2. Selected business cases

The selection of V2X services to develop the business models must take into account the existence of a market, economic attractiveness, energy intensity, trials and its suitability for either residential users (RUs) and/or EV fleets.

PA is selected because Denmark revised the time of use (ToU) tariffs in 2023, putting an increased cost on consumption in peak hours. Dynamic pricing makes these services economically attractive, and in Denmark, dynamic electricity prices for end-users are largely rolled-out already. Energy intensity of arbitrage operations is estimated to be medium as it is constrained by local consumption, however, it is higher when also exporting electricity back into the grid. In addition, various investigations highlight the significant economic potential of V2G offering frequency containment reserves (FCRs) [8,10,34]. In Denmark, this service is split into frequency containment reserve for normal operation (FCR-N) and frequency containment reserve for disturbances (FCR-D). FCR-N continuously stabilizes the frequency within the band between 49.9 and 50.1 Hz. In FCR-D, upregulation stabilizes occasional sudden frequency drops below 49.9 Hz, and is procured separate from downregulation, which stabilizes frequency surges above 50.1 Hz. FCR products are procured up until one day-ahead in a joint Danish/Swedish regulation/balancing market on an hourly level. However, the service is only suitable for EV fleets due to the availability and minimum capacity required to participate in the market. According to [35], primary frequency control has the highest activation and economic potential. In the scope of this study, FCR-D is selected over FCR-N, because a high energy intensity is connected with the latter. Despite lower prices, FCR-D upregulation is chosen to investigate the trade-off with battery degradation because the upregulation service motivates a relatively high SOC for ensuring vehicle discharge availability and large bidding capacity.

Following the identification of the most promising V2X services, the design of business models serves as a framework for developing optimal operational strategies. The primary goal of the models is to reduce overall electricity costs, either by achieving cost savings or generating revenue. Hereby, it must always be ensured that the EVs still satisfy the driving demands of their users. Fig. 1 presents the resulting four investigated business models: (a) V2H, (b) Residential V2G, (c) Fleet V2G and (d) Fleet V2G plus FCR-D.

In V2H, a household can only draw power from the grid. The household owns an EV which is connected to the house through a bidirectional charger, allowing it not only to charge but also to discharge and supply household consumption while it is parked at home, see (a) of Fig. 1. The net electricity consumption from the grid is billed by the electricity retailer, which purchases energy from the wholesale electricity market. The cost for electricity consumption is equivalent to the hourly spot price plus additional components arising from TSO tariffs, distribution system operator (DSO) tariffs and state taxes. The bidirectional ability of the EV can achieve cost savings by optimizing the time at which the household draws energy from the power grid, taking advantage of varying ToU tariffs, consisting of low, high and peak price periods, as well as spot price variations.

Residential V2G refers to the case where a household is able to both draw power from and feed it into the grid. The objective, agents and assets involved are identical to V2H. However, a production meter is added and the electricity retailer is replaced by a production electricity supplier (PES) as seen in (b) of Fig. 1. The PES provides the consumer with power and sells their (over)production. The PES aggregates consumers' production, which otherwise would be too low to participate in the wholesale electricity market. Still, the business model focuses on a single household, highlighted in Fig. 1. In addition to managing household consumption, the EV charges surplus energy during time periods of low electricity prices and sells it when prices are high. The selling price of the energy fed back into the grid is the spot price minus additional fees from the PES services, TSO producer tariffs and DSO producer tariffs, while the cost of electricity consumed is the same as in V2H.

Fleet V2G alludes to the PA done by an EV fleet connected by bidirectional chargers to a point of common coupling (PCC), enabling grid connection, as shown in (c) of Fig. 1. The PCC connects photovoltaic (PV) panels, a commercial building and the EV depot. The EV fleet manager is responsible for all these assets. The EV fleet parked at the depot can charge or discharge to cover building consumption or use the PV production. Otherwise, surplus energy from the EV fleet or PV production can be fed into the grid to generate revenue. A PES is assumed to handle the electricity transactions, due to the time and cost savings associated with its specialized service. Thus, the same cost and revenue concepts apply as described for Residential V2G.

The Fleet V2G plus FCR-D business model is an extension of the Fleet V2G where the EV fleet additionally offers FCR-D up reserves in the regulating market. As seen in (d) of Fig. 1, access to this market is considered through an aggregator as the balance service provider (BSP), who disposes of specific target consumption/production to provide the service. In the case of FCR-D up the fleet is discharged, thus enough energy has to be available in the EVs' batteries. Reserved capacity is paid as bid but there is no payment for the delivered energy. All other costs mentioned for Fleet V2G apply plus the aggregator imposed service fees.

3. Methodology

To evaluate the techno-economic impact of the four presented business models, associated mathematical optimization models with the objective of minimizing overall costs are developed. First, this section explains the proposed method for battery degradation costs modeling. Afterwards, the overall set-up of the models as well as the implemented objective functions and constraints are described. A detailed nomenclature can be found in the Appendix.

3.1. Battery degradation cost

A reduction in state of health (SOH) occurs due to both cycle and calendar degradation. Cycle degradation is caused by charging and discharging the battery. The total energy throughput measured in full equivalent cycles (FECs) is a good estimate for the cost calculation [36]. Consequently, the cost per FEC α^{cyc} is modeled in Eq. (1). Here, $\alpha^{battery}$ represents the battery's cost per kWh, c represents its nominal capacity, c^{useful} assumes a useful battery capacity lifetime for vehicular application and δ^{cyc} estimates the SOH loss every FEC. The value for δ^{cyc} is specified in Section 4.1.

$$\alpha^{cyc} = \delta^{cyc} \cdot \frac{c \cdot \alpha^{battery}}{c - c^{useful}} \tag{1}$$

Calendar degradation comprises all aging processes independent of cycling. For lithium-ion cells high levels of SOC and high temperatures accelerate calendar aging. Plateau regions exist where the capacity fade is similar [37]; this feature makes it appropriate to utilize a semi-empirical model for calendar degradation modeling. Thus, a base calendar degradation rate δ^{cal}_{ba} is linearly estimated over the years from [38] at 65% SOC and an additional increase in degradation δ^{cal}_{ad} is taken at 75% SOC, both excluding the first year where degradation is higher compared to consecutive years. These rates are also differentiated for summer at 25 °C and winter at 10 °C. Due to the variable rate of calendar degradation, it is essential to quantify the cost α^{cal} per SOH loss, as demonstrated in Eq. (2).

$$\alpha^{cal} = \frac{c \cdot \alpha^{battery}}{c - c^{useful}} \tag{2}$$

Notably, battery degradation is quantified as a cost but is not accounted for physically, as it is considered negligible in terms of reduced usable capacity over one year [38].

3.2. Model set-up

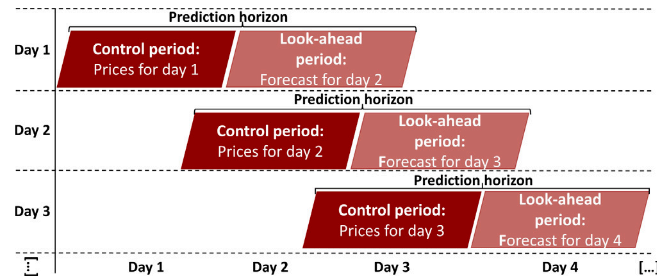

Fig. 2. Principle of the rolling horizon with persistence forecast for prices.

While the overall optimization is set for a whole year, the model runs day by day in a rolling-horizon fashion to limit its foresight, as illustrated in Fig. 2. On the initial date, the optimization is based on historical prices of this respective day. This is called the *control period*, while the *look-ahead period* includes the whole next day. Applying a persistence forecast, the prices are predicted to be the same on the next consecutive day. The model then sets the decision variables for the first and second day, using the actual and predicted information for these days. Thus, the *prediction horizon* on each day is 48 h. Hereby, the constraints define the boundaries of the values which the decision variables can take to achieve the smallest possible outcome for the objective function. The values of the decision variables are saved when the optimization for the first day is finished. Then, the model moves on to the second day and gets the actual data for the second and the predicted data for the third day. The optimization is executed based on the new information, running in a loop for each day of the year. However, only the values of the *control period* are later considered for the results. Only the price and FCR-D parameters are implemented with the persistence forecast. The foresight for the other parameters, e.g. household consumption, is also restricted to two days using the rolling horizon. Yet, the actual values are used for the *control* and the *look-ahead period*.

3.3. V2H

The objective function of the optimization for V2H is divided in three summations, as seen in Eq. (3). The first one represents arising costs for electricity consumption from the grid $E^{grid}_{t,u}$, considering the consumer electricity price $\pi^{el}_{d,t}$. The other summations determine costs resulting from calendar and cycle battery degradation. The former considers the calendar capacity loss $\delta^{cal}_{d,t,u}$ and associated costs α^{cal} (see Section 3.1).

$$\min_{E^{grid}_{t,u},E^{char}_{t,u},E^{dis}_{t,u},\delta^{cal}_{d,t,u}} \underbrace{\sum_{t\in T,u\in U} E^{grid}_{t,u}\cdot \pi^{el}_{d,t}}_{\text{Electricity cost}} + \underbrace{\sum_{t\in T,u\in U} \delta^{cal}_{d,t,u}\cdot\alpha^{cal}}_{\text{Calendar degradation cost}} + \underbrace{\sum_{u\in U} \frac{\sum_{t\in T} E^{char}_{t,u}+E^{dis}_{t,u}+\kappa_{d,t,u}}{2\cdot c}\cdot\alpha^{cyc}}_{\text{Cycle degradation cost}} \tag{3}$$

To compute the cycle battery degradation the driving consumption $\kappa_{d,t,u}$ is added to the energy throughput from charging and discharging the EV, $E^{char}_{t,u}$ and $E^{dis}_{t,u}$. By dividing the total energy throughput by twice the battery capacity c the FECs are obtained which are then multiplied by associated costs α^{cyc}.

The following constraints define the system boundaries. Eq. (4) presents the energy balance which ensures that energy charged to the EV $E^{char\_pcc}_{t,u}$ and discharged from it $E^{dis\_pcc}_{t,u}$, as well as the household consumption $\gamma_{d,t}$ are reflected in the energy drawn from the grid $E^{grid}_{t,u}$.

$$E^{grid}_{t,u} \geq \gamma_{d,t} + E^{char\_pcc}_{t,u} - E^{dis\_pcc}_{t,u} \quad \forall\, t\in T,\; u\in U \tag{4}$$

The following four constraints regard the charging and discharging of the EV. In Eq. (5), the possible charging steps P^{char}_{p} are associated with an efficiency η^{char}_{p}. To ensure the charging and discharging granularity being independent of time steps dictated by input parameters, e.g. spot prices, the variable $\beta^{char}_{t,p,u}$ is introduced. It specifies how many 10 min charging windows are assigned to different charging steps for each hour t and user u, while the scalar ω defines the number of charging slots in an hour. Taking the sum of all charging steps $p\in P$, thus, results in the total energy $E^{char}_{t,u}$ charged to the EV. Eq. (6) applies the same logic to the discharging process.

$$E^{char}_{t,u} = \sum_{p\in P} P^{char}_{p}\cdot\eta^{char}_{p}\cdot\frac{\beta^{char}_{t,p,u}}{\omega} \quad \forall\, t\in T,\; u\in U \tag{5}$$

$$E^{dis}_{t,u} = \sum_{p\in P} \frac{P^{dis}_{p}}{\eta^{dis}_{p}}\cdot\frac{\beta^{dis}_{t,p,u}}{\omega} \quad \forall\, t\in T,\; u\in U \tag{6}$$

In the same way, Eqs. (7) and (8) are established. The only difference are the efficiencies, as $E^{char\_pcc}_{t,u}$ and $E^{dis\_pcc}_{t,u}$ represent the charging and discharging energy at the PCC of the household and the grid:

$$E^{char\_pcc}_{t,u} = \sum_{p\in P} P^{char}_{p}\cdot\frac{\beta^{char}_{t,p,u}}{\omega} \quad \forall\, t\in T,\; u\in U \tag{7}$$

$$E^{dis\_pcc}_{t,u} = \sum_{p\in P} P^{dis}_{p}\cdot\frac{\beta^{dis}_{t,p,u}}{\omega} \quad \forall\, t\in T,\; u\in U \tag{8}$$

To implement the charging windows, three more constraints are needed. To ensure that the EV can only be charged or discharged within an hour, $\rho^{char}_{t,u}$ and $\rho^{dis}_{t,u}$ are established. Thus, in Eq. (9) the sum of these binary variables is confined to be less or equal to the binary variable $\theta_{d,t,u}$. The latter specifies if the EV is available at home.

$$\rho^{char}_{t,u} + \rho^{dis}_{t,u} \leq \theta_{d,t,u} \quad \forall\, t\in T,\; u\in U \tag{9}$$

Eqs. (10) and (11) ensure that the sum over all charging steps p of $\beta^{char}_{t,p,u}$ can take the maximum value of ω, meaning that all charging windows are covered by the charging process. Similarly, the sum over all discharging steps p of $\beta^{dis}_{t,p,u}$ can also take a value lower than ω if not all time slots are needed to discharge.

$$\sum_{p\in P} \beta^{char}_{t,p,u} \leq \omega\cdot\rho^{char}_{t,u} \quad \forall\, t\in T,\; u\in U \tag{10}$$

$$\sum_{p\in P} \beta^{dis}_{t,p,u} \leq \omega\cdot\rho^{dis}_{t,u} \quad \forall\, t\in T,\; u\in U \tag{11}$$

After specifying all power and energy flows, the SOC of the EV battery represented by $SOC_{d,t,u}$ has to be defined. Eqs. (12) and (13) set the minimum and maximum boundaries of the SOC. For the upper limit, the decision variable $y_{d,t,u}$ allows to operate below SOC^{max} or up until the battery's capacity. If the battery operates above the defined threshold, $y_{d,t,u}$ assumes a true value for that hour.

$$SOC^{min} \leq SOC_{d,t,u} \quad \forall\, t\in T,\; u\in U \tag{12}$$

$$SOC_{d,t,u} \leq c\cdot y_{d,t,u} + SOC^{max}\cdot\left(1-y_{d,t,u}\right) \quad \forall\, t\in T,\; u\in U \tag{13}$$

Eqs. (14) and (15) specify the incurred calendar degradation $\delta^{cal}_{d,t,u}$. Hereby, seasonal variations in degradation are considered and base and additional battery degradation are distinguished. The latter results from exceeding SOC^{max}.

$$\delta^{cal}_{d,t,u} \geq \delta^{cal}_{ba,s} + \delta^{cal}_{ad,s}\cdot y_{d,t,u} \quad \forall\, t\in T,\; u\in U,\; d\in S \tag{14}$$

$$\delta^{cal}_{d,t,u} \geq \delta^{cal}_{ba,w} + \delta^{cal}_{ad,w}\cdot y_{d,t,u} \quad \forall\, t\in T,\; u\in U,\; d\in W \tag{15}$$

At last, the SOC needs to be computed for each hour t and user u in Eq. (16). The first of the three if-statements behind the curly brackets ensures that the last SOC of the previous day $SOC_{d-1,24,u}$ is considered for the first hour of each day. However, on the first day of the simulation, there is no day to refer back to, so the second if-statement defines that SOC^{min} is used for the first hour. For the rest of the hours of all following days, the SOC of the previous hour $SOC_{d,t-1,u}$ is considered. The charged and discharged energy $E^{char}_{t,u}$ and $E^{dis}_{t,u}$, respectively, are added or subtracted to the previous SOC, to account for the increased or decreased energy in the EV battery. Furthermore, $\kappa_{d,t,u}$ is deducted to consider the driving consumption of the EV. Thus, $SOC_{d,t,u}$ represents the energy content of the battery at the end of each hour t.

$$\begin{aligned} SOC_{d,t,u} = &\begin{cases} SOC_{d-1,24,u} & \text{, if } d\geq 2\wedge t=1 \\ 0 & \text{, if } d<2\wedge t>1 \end{cases} \\ &+\begin{cases} SOC^{min} & \text{, if } d=1\wedge t=1 \\ 0 & \text{, if } d>1\wedge t>1 \end{cases} \\ &+\begin{cases} SOC_{d,t-1,u} & \text{, if } t\geq 2 \\ 0 & \text{, if } t<2 \end{cases} \\ &+E^{char}_{t,u} - E^{dis}_{t,u} - \kappa_{d,t,u} \quad \forall\, t\in T,\; u\in U \end{aligned} \tag{16}$$

3.4. Residential V2G

The objective function of Residential V2G contains the same summations as Eq. (3). However, to include the grid feed-in, two terms are added as formulated in Eq. (17).

$$\begin{aligned} \min_{E^{grid}_{t,u},E^{feedin}_{t,u},E^{char}_{t,u},E^{dis}_{t,u},\delta^{cal}_{d,t,u}} &\underbrace{\sum_{t\in T,u\in U} E^{grid}_{t,u}\cdot\pi^{el}_{d,t}}_{\text{Electricity cost}} - \underbrace{\sum_{t\in T,u\in U} E^{feedin}_{t,u}\cdot\pi^{spot}_{d,t}}_{\text{Feed-in revenue}} \\ &+ \underbrace{\sum_{t\in T,u\in U} E^{feedin}_{t,u}\cdot\left(\tau^{TSO}+\tau^{PES}+\tau^{DSO}\right)}_{\text{Feed-in cost}} \\ &+ \underbrace{\sum_{t\in T,u\in U} \delta^{cal}_{d,t,u}\cdot\alpha^{cal}}_{\text{Calendar degradation cost}} + \underbrace{\sum_{u\in U} \frac{\sum_{t\in T} E^{char}_{t,u}+E^{dis}_{t,u}+\kappa_{d,t,u}}{2\cdot c}\cdot\alpha^{cyc}}_{\text{Cycle degradation cost}} \end{aligned} \tag{17}$$

The objective function minimizes electricity costs, so the revenue generated from selling electricity to the grid is deducted from the cost. Therefore, the spot price $\pi_{d,t}^{spot}$ is multiplied with $E_{t,u}^{feedin}$. However, costs arise for each kWh fed into the grid. They are represented by multiplying $E_{t,u}^{feedin}$ with all arising tariffs, τ^{TSO}, τ^{PES} and τ^{DSO}, and adding it to the objective function.

$E_{t,u}^{feedin}$ is furthermore included in the energy balance constraint, enabling $E_{t,u}^{dis\_pcc}$ to be greater than the demand $\gamma_{d,t}$. Therefore, it is subtracted on the grid side, as seen in Eq. (18).

$$E_{t,u}^{grid} - E_{t,u}^{feedin} \geq \gamma_{d,t} + E_{t,u}^{char\_pcc} - E_{t,u}^{dis\_pcc} \quad \forall\ t \in T,\ u \in U \tag{18}$$

3.5. Fleet V2G

Continuing on to the EV fleet models, once more the overall goal of the optimization models is to minimize electricity costs. Here, E_t^{grid} and E_t^{feedin} are only dependent on the time steps t, combining all consumption and feed-in at the PCC. The variables representing charging and discharging, $E_{t,v}^{char}$ and $E_{t,v}^{dis}$, are now taken per vehicle v. Otherwise, the terms represent the same costs as in the RUs' models.

$$\begin{aligned}\min_{E_t^{grid},E_t^{feedin},E_{t,v}^{char},E_{t,v}^{dis},\delta_{t,v}^{cal}} &\underbrace{\sum_{t\in T} E_t^{grid}\cdot \pi_{d,t}^{el}}_{\text{Electricity cost}} - \underbrace{\sum_{t\in T} E_t^{feedin}\cdot \pi_{d,t}^{spot}}_{\text{Feed-in revenue}} \\ &+ \underbrace{\sum_{t\in T} E_t^{feedin}\cdot(\tau^{TSO}+\tau^{PES}+\tau^{DSO})}_{\text{Feed-in cost}} \\ &+ \underbrace{\sum_{v\in V}\frac{\sum_{t\in T}E_{t,v}^{char}+E_{t,v}^{dis}+\kappa_{d,t}}{2\cdot c}\cdot\alpha^{cyc}}_{\text{Cycle degradation cost}} + \underbrace{\sum_{t\in T,v\in V}\delta_{t,v}^{cal}\cdot\alpha^{cal}}_{\text{Calendar degradation cost}}\end{aligned} \tag{19}$$

To implement the PCC, the energy balance constraint is adjusted, as displayed in Eq. (20). The difference of E_t^{grid} and E_t^{feedin} needs to satisfy the demand $\gamma_{d,t}$ and the sum of all charging $E_{t,v}^{char\_pcc}$. Following load convention, $PV_{d,t}$ is deducted from all demands, as well as the sum of all discharging $E_{t,v}^{dis\_pcc}$.

$$\begin{aligned}E_t^{grid} - E_t^{feedin} \geq\ &\gamma_{d,t} - PV_{d,t} \\ &+ \sum_{v\in V}\left(E_{t,v}^{char\_pcc} - E_{t,v}^{dis\_pcc}\right) \quad \forall\ t\in T\end{aligned} \tag{20}$$

To match the new set of vehicles v, all remaining constraints are adjusted accordingly. For an example, refer to Eq. (21).

$$E_{t,v}^{char} = \sum_{p\in P^{sc}} P_p^{char}\cdot\eta_p^{char}\cdot\frac{\beta_{t,p,v}^{char}}{\omega} \quad \forall\ t\in T, v\in V \tag{21}$$

3.6. Fleet V2G + FCR-D

In the case of offering FCR-D up reserves, sufficient energy has to be available in the EVs' batteries to discharge upon request and still align with the goal to minimize costs. In Eq. (22) the costs for electricity drawn from the grid, grid feed-in and calendar and cycle degradation are added up. The revenue from the grid feed-in and the FCR-D up provision is, however, subtracted to reduce overall costs. Hereby, the reserved power P_t^{res} is multiplied with the FCR-D price $\pi_{d,t}^{FCR-D}$.

$$\begin{aligned}\min_{E_t^{grid},E_t^{feedin},E_{t,v}^{char},E_{t,v}^{dis},\delta_{t,v}^{cal}} &\underbrace{\sum_{t\in T} E_t^{grid}\cdot \pi_{d,t}^{el}}_{\text{Electricity cost}} - \underbrace{\sum_{t\in T} E_t^{feedin}\cdot \pi_{d,t}^{spot}}_{\text{Feed-in revenue}} - \underbrace{\sum_{t\in T} P_t^{res}\cdot \pi_{d,t}^{FCR-D}}_{\text{FCR-D revenue}} \\ &+ \underbrace{\sum_{t\in T} E_t^{feedin}\cdot(\tau^{TSO}+\tau^{PES}+\tau^{DSO})}_{\text{Feed-in cost}} \\ &+ \underbrace{\sum_{v\in V}\frac{\sum_{t\in T}E_{t,v}^{char}+E_{t,v}^{dis}+\kappa_{d,t}}{2\cdot c}\cdot\alpha^{cyc}}_{\text{Cycle degradation cost}} + \underbrace{\sum_{t\in T,v\in V}\delta_{t,v}^{cal}\cdot\alpha^{cal}}_{\text{Calendar degradation cost}}\end{aligned} \tag{22}$$

In addition to all constraints used in the model of Fleet V2G, several constraints are added to implement the provision of FCR-D up. In Eq. (23) the discharging power is summed for all vehicles v. By setting one discharging step p to 1 for each vehicle v, the binary $res_{t,p,v}^{up}$ indicates the individually selected discharging step. Summing the product of these variables for all vehicles and discharging steps results in the total discharging power, which is stored in P_t^{res}.

$$P_t^{res} \leq \sum_{v\in V,p\in P^{sd}} \frac{P_p^{dis}\cdot res_{t,p,v}^{up}}{\eta_p^{dis}} \quad \forall\ t\in T \tag{23}$$

Since only one discharging step p should be selected for each vehicle v for each hour, the sum over all discharging steps p is set to be less than or equal to 1 in Eq. (24).

$$\sum_{p\in P^{sd}} res_{t,p,v}^{up} \leq 1 \quad \forall\ t\in T,\ v\in V \tag{24}$$

However, to provide the power sold for FCR-D, the vehicles have to be at the depot. Consequently, the volume $vol_{d,t}^{FCR-D}$ is multiplied by the binary availability variable $\theta_{d,t}$, which assumes the value of 1 when the EVs are present at the depot. Furthermore, the market share χ is included in the multiplication, so that for each time step t the value of the FCR-D power sold cannot exceed the maximum defined market share of the total volume of the reserve purchased by the Danish TSO Energinet. The market share χ represents a limit to the attainable FCR-D up regulation by sizing an adequate volume that could be secured through competitive market bids and delivered certainly by the fleet. It is therefore possible to assume that all P_t^{res} which the model decides to sell is purchased in the market. In reality, the TSO decides which FCR-D offers to buy to fulfill its needs.

$$P_t^{res} \leq \theta_{d,t}\cdot vol_{d,t}^{FCR-D}\cdot\chi \quad \forall\ t\in T \tag{25}$$

Furthermore, a unit needs to be able to provide its power sold for FCR-D in the ancillary services market for at least 20 min. Yet, the time steps used in the optimization models are hours. Consequently, the resulting energy reserve E_t^{res} needed for an hour in which FCR-D provision is considered is calculated as shown in Eq. (26).

$$E_t^{res} \geq P_t^{res}\cdot\frac{1}{3} \quad \forall\ t\in T \tag{26}$$

In Eq. (27) the needed energy reserve is related the storage of the EV fleet. Hereby, the sum of SOC^{min} for all vehicles v is added to the E_t^{res} provided by all EVs, ensuring that the EV fleet keeps the defined minimum SOC and stores enough energy to fulfill the FCR-D requirement. Thus, the sum of the $SOC_{d,t,v}$ over the vehicles at each hour must be greater than or equal to the aforementioned term.

$$\sum_{v\in V} SOC_{d,t,v} \geq E_t^{res} + \sum_{v\in V} SOC^{min} \quad \forall\ t\in T \tag{27}$$

Note that in the optimization model, the energy discharged from the EV fleet in case of activation of the sold FCR-D up reserve is not considered. Only about 1% of the time the Nordic power system frequency falls below 49.9 Hz, so the energy invested in actually providing FCR-D is negligible, as specified by [39]. Thus, it is not implemented in the optimization model.

3.7. Computational setup

The model is run in an hourly resolution in a day-by-day rolling horizon sequence for a full year. It is implemented in the JuMP environment of the programming language Julia v1.6.7, which is commonly used among research institutions and for energy system modeling [40]. The model was optimally solved with Gurobi v11.0.1 using Intel Core i5-1345U processor with a time limit of 2 min and an average quality of the solution of 0.01%. Depending on the case, the mixed-integer linear program comprises at most 62,592 constraints and 158,592 variables of which 52,800 are binaries.

4. Case study

4.1. Residential business cases

For the optimization models, several inputs and parameters are selected to characterize the components outlined in the residential business cases. The hourly availability of the EV $\theta_{d,t,u}$ is defined based on three different RU usage patterns. First, the *on-site* user is commuting to and working at its workplace every weekday from 7 am til 5 pm. Second, the *remote* user is always working from home, however, they leave the house every day for errands. Therefore, their EV is considered unavailable from 9 to 11 pm on Monday and Tuesday and 9 to 11 am on Wednesday and Thursday. Third, the *hybrid* user is established as a mixture of the other two types based on [41]. They behave like the *on-site* user on Monday, Tuesday and Wednesday and like the *remote* user on Thursday and Friday. The weekend pattern is the same for all three user types. On Saturday the EV is away from 9 am until 3 pm, while on Sunday it is at home the whole day. For simplicity, every week is considered to be the same.

As an exemplary EV the Nissan Leaf is selected. This model features a usable battery capacity c of 59 kWh and a nominal consumption of 172 Wh/km [42]. Due to outdoor temperatures, consumption varies during the year. As winter and summer are defined for the ToU tariffs, October-March and April-September, respectively, this is taken as a Ref. [43]. Dost et al. [44] determined nominal consumption to be 29% lower in summer and 18% higher in winter. An estimate of the driving consumption $\kappa_{d,t,u}$ is derived from the average distance and duration of commuting in the Danish region of Zealand [45], spread over all hours the EV is away according to the availability of each RU. The commuting distance is 57.4 km with a duration of nine hours. However, only 10 km are assumed for the two-hour slots of the *remote* and *hybrid* user. Lastly, the six hour trip on Saturday is considered to cover 100 km.

Typical EV charger power ranges between 3.7 kW to 22 kW. An average maximum charging power P^{char} of 6 kW is considered suitable for general household demand. The charging and discharging efficiency curve is assumed similar to the Fronius Symo 6.0-3-M inverter [46].

To incorporate the cost of battery degradation, the battery cost of 180 €/kWh is assumed with a lifetime for vehicular application determined by the point at which it experiences a 20 to 30 $\%^{SOH}$ loss and needs replacement [47]. In this regard, c^{useful} is set to 70% of the nominal capacity. Then, battery degradation costs α^{cyc} and α^{cal} can be determined. SOH specifies the state of the capacity with respect to its original amount, so 100% is assumed as the initial value. Based on [47], a 3 $\%^{SOH}$ loss for each 1,000 FECs is considered for cycle degradation. Moreover, 65% is set up as the SOC^{max} in accordance to calendar degradation plateau regions discussed in Section 3.1. Meanwhile, 30% is established as SOC^{min} [48] to address user concerns of inconvenience and range anxiety.

Besides the aforementioned inputs, time series data from the year 2023 are considered for the spot price and household demand. The spot prices for the bidding zone DK2 $\pi^{spot}_{d,t}$ are taken from Nordpool for every hour of the year [49]. The electricity price $\pi^{el}_{d,t}$ is derived from spot prices plus additional tariffs. The TSO tariffs τ^{TSO} are defined by Energinet for 2023 and the DSO tariffs τ^{DSO} are those applicable as of October 2023 for customers in category C, according to DSO Cerius. For V2G operation, the PES tariff τ^{PES} 0.0054 €/kWh is taken from Nettøpower, a registered PES in Denmark [50]. Although there are financial incentives for EVs in Denmark, such as electricity tax refunds or exemptions [51], the case study applies the full tax of 0.102 €/kWh because these incentives do not apply to the business models under consideration. For the household demand $\gamma_{d,t}$, the hourly average demand of Danish households from Zealand in kWh is specified for each month, as presented by the DSO Radius [52]. The data distinguishes between weekdays and weekends, and corresponds to detached houses without electric heating. They represent the majority and are expected to have private charging points and self-supply capabilities.

4.2. Fleet business cases

The EV fleet to consider originates from an e-mail interview conducted with Amager Ressourcecenter (ARC), a waste management company in Copenhagen operating a fleet of electric refuse trucks. ARC's fleet consists of 100 trucks each with 300 kWh of battery capacity c, either from Volvo or Scania. Hereby, a theoretical EV fleet possessing identical attributes to the actual fleet is studied. ARC's charging station consists of 100 ABB chargers with charging capacity P^{char} of 100 kW and 20 kW. For the case study, it is assumed they have 100 kW bidirectional charging/discharging capability. The availability $\theta_{d,t,v}$ and driving consumption $\kappa_{d,t,v}$ of the fleet come from the refuse trucks' schedule. The trucks are away from the depot from 6 am until 5 pm, each covering 75 km per day while consuming 170 kWh/day. There is no difference between the vehicles, but the consumption varies in summer and winter as specified in Section 4.1.

The time series determining the PV production $PV_{d,t}$ and demand $\gamma_{d,t}$ of a potential office building, have their origin in the data from Campus Bornholm from the projects of EV4EU [53] and INSULAE [54]. The dataset from 2018 is adjusted to align with 2023. The building has a peak demand of 276 kW and a yearly consumption of 550 MWh. Moreover, the PV generation, from a 61 kWp system [55], is scaled up to 450 kWp to accommodate the estimated depot area suitable for a PV installation. At last, time series for FCR-D prices $\pi^{FCR-D}_{d,t}$ and volumes $vol^{FCR-D}_{d,t}$ in 2023 are retrieved from the data hub of the TSO Energinet [56]. From the volume sold, a hypothetical market share χ of 5% is assumed to account for a potential prospective contribution from flexible resources. This share is comparable to the contribution of batteries and flexible resources to the added FCR-D upregulation capacity in 2023. In the coming years, procurement from these technologies is expected to rise as the combined Danish-Swedish demand for 600 MW of FCR-D upregulation grows due to the accelerated energy transition into intermittent renewable based power system [57]. Previous inputs, such as battery degradation, grid feed-in costs, spot price, etc. are the same and not revised in this section. Only DSO tariffs change to match a consumer of category A-low (connection at 10 kV side of a substation).

5. Results

The results are presented in two subsections: Section 5.1 is on RU business cases and Section 5.2 on EV fleet business cases. Results common to both models within a section are discussed, before moving on to relevant individual results. To put the results in perspective and to extract potential benefits of V2X services, a unidirectional case is created. Hereby, the objective, agents and assets involved remain the same as described in Section 2, except that the EVs do not have the ability to discharge power.

Table 1
Yearly results of residential cases.

		Unidirectional			V2H			Residential V2G		
		Remote	Hybrid	On-site	Remote	Hybrid	On-site	Remote	Hybrid	On-site
Net profit	[€] [%] vs. uni	−1909	−2238	−2453	−1710 10%	−2067 8%	−2296 6%	−1705 11%	−2064 8%	−2293 7%
Feed-in profit	[€] [%] vs. uni	–	–	–	–	–	–	21	18	18
E^{grid}	[kWh] [%] vs. uni	5290	6598	7413	5401 2%	6688 1%	7490 1%	5482 4%	6754 2%	7555 2%
E^{grid_feedin}	[kWh] [%] vs. uni	–	–	–	–	–	–	84	69	67
E^{char_pcc}	[kWh] [%] vs. uni	1198	2506	3321	3607 201%	4456 78%	4985 50%	3703 209%	4526 81%	5056 52%
E^{dis_pcc}	[kWh] [%] vs. uni	–	–	–	2305	1866	1592	2397	1934	1661
Self-sufficiency	[%] [%] vs. uni	–	–	–	30%	22%	17%	30%	22%	17%
SOH loss	[%] [%] vs. uni	1.06	1.12	1.16	1.18 12%	1.22 10%	1.25 9%	1.18 12%	1.22 10%	1.25 9%

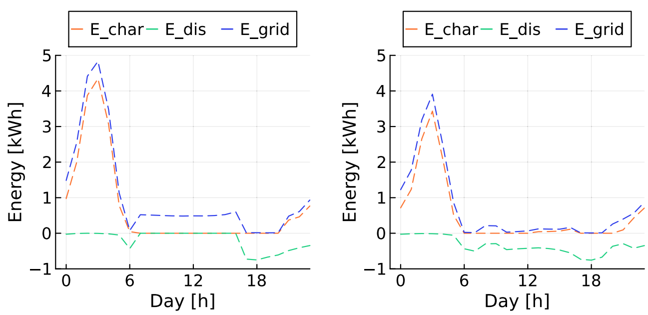

(a) On-site user (b) Remote user

Fig. 3. Electricity drawn from the grid and charging/discharging behavior on weekdays in winter.

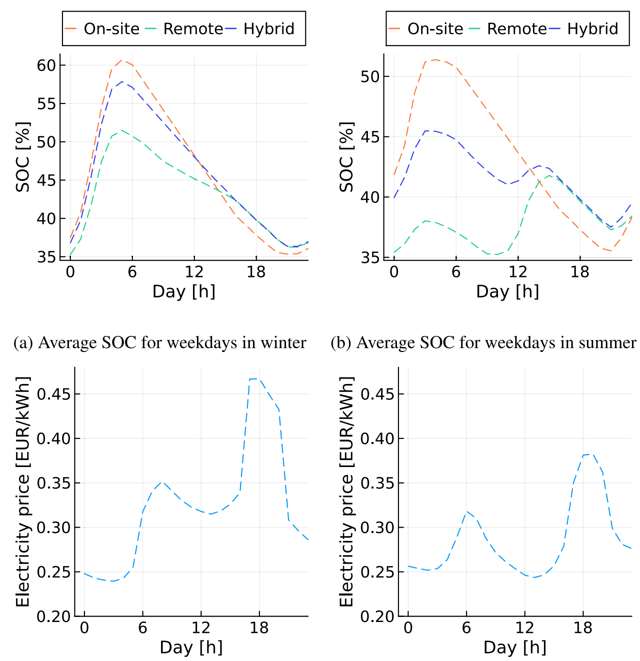

(a) Average SOC for weekdays in winter (b) Average SOC for weekdays in summer

(c) Average electricity prices on weekdays in winter (d) Average electricity prices on weekdays in summer

Fig. 4. Average SOC of each user and electricity prices for weekdays in summer and winter.

5.1. Residential users

PA as a strategy for cost reduction of RUs yields the yearly results shown in Table 1. It is possible to either cover on-site consumption in V2H or sell surplus energy charged back into the grid in V2G. Consequently, the net profit accounts for the costs of electricity consumption and battery degradation, while also incorporating the feed-in profit as a potential mitigating element. The unidirectional case is presented as a baseline against which cost savings and other results can be compared.

Overall, the net profits in the bidirectional cases are higher than in the unidirectional case. On average, V2H achieves 174 € and Residential V2G 179 € yearly cost savings. Among the user categories, the range of cost savings spans from 6% to 11% depending on the user's flexibility. The *remote* user achieves the highest savings and the *on-site* user the lowest. The reason is that the *on-site* user has the least flexibility due to its strong demand for driving on weekdays. Still cost savings can be achieved, because the highest electricity prices typically occur while the EV is present.

Energy drawn from the grid is stored first in the EV and then discharged when convenient. For this reason, the increase in E^{grid} is not proportional to E^{char_pcc}, highlighting the opportunity for PA. The charging and discharging operation in both bidirectional cases is similar for every weekday. Fig. 3 illustrates the average operation for weekdays in winter of V2H for the user profiles with low and high cost reductions. Both have a peak demand of 4–5 kWh/h between 12 am and 6 am, where the electricity prices are low, coinciding with the EV charging. At the peak electricity price at 6 pm, energy is never drawn from the grid. In these hours, household demand is satisfied by discharging the EV. Winter weekends follow a similar pattern.

In summer, the operation remains mostly the same. However, the remote user has a second charging window around 1 pm during weekdays. Fig. 4 shows the rise of the SOC for each user. This coincides with the afternoon dip in electricity prices. In summer weekends there is not a clear pattern, as the flexibility of the RUs increases and the difference of electricity prices within a day decreases. In general, the EV is charged right before it is needed when there is an opportunity of a price decline. The charging/discharging decisions are not limited by energy losses due to lower efficiencies at low power steps.

Indeed, the utilization of the EV rose from unidirectional to bidirectional operation. For instance, the E^{char_pcc} increased, ranging from half to double depending on user flexibility. The increase in energy charged

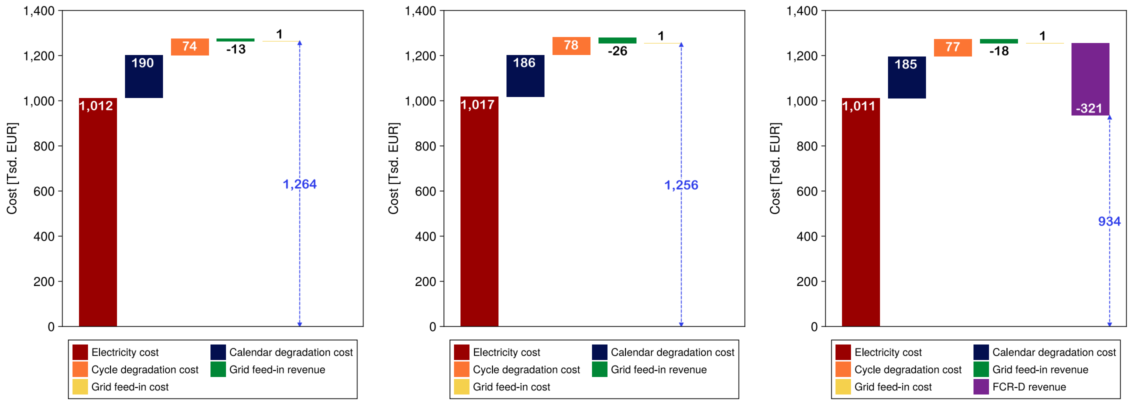

(a) Unidirectional case (b) Fleet V2G (c) Fleet V2G + FCR-D

Fig. 5. Structure of yearly costs.

is later discharged to satisfy household consumption or feed back into the grid. Here, self-sufficiency refers to the total local consumption, EV charging and household demand, which is not supplied by the grid but covered locally [58]. The results show no relevant difference between V2H and V2G, both focus on satisfying household demand. Electricity feed-in happens rarely, only when the price difference is at least 0.036 €/kWh, between the selling and charging price, to overcome incurred costs. This happened 2.5% of the days in the modeled year.

As battery usage increased by E^{char_pcc} and E^{dis_pcc}, degradation also increased. The SOH loss increased by 9% to 12% from unidirectional to bidirectional operation. The optimal bidirectional operation of the battery is reflected on the average SOC in Fig. 4. Calendar degradation stays almost the same between unidirectional and bidirectional operation because the threshold for increased degradation is not crossed. Thus, the increase in the SOH loss is due to cycle degradation. The model sees no restriction in cycling the battery for bidirectional purposes, as long as it is economically viable and operated within the normal range of SOC.

Overall, V2H and V2G perform very similar. The small advantage of the latter is lost because consumers who count as auto-producers in Residential V2G are subject to a yearly one-time payment of 13.4 € due to the network and availability subscriptions. Transitioning from unidirectional to bidirectional operation requires an additional investment. For example, 945 € for openWB chargers [59,60] or 3,475 € for Wallbox chargers [61,62]. The simple payback period is between 5 to 6.6 years or 18 to 23 years, depending on the charger. On the lower range, V2H is suitable for RUs in terms of economic feasibility and actual implementation. There is no reason to argue for the implementation of Residential V2G over V2H.

5.2. Fleet vehicles

The yearly results from the optimization models are illustrated in Fig. 5, breaking down the different components of the net profit. Here, costs add up to the total structure, whereas revenues reduce it. Moreover, the double arrowheads indicate the net profit of each. Compared to the unidirectional case, Fleet V2G and V2G plus FCR-D result in cost savings. Notably, V2G plus FCR-D achieves cost savings of 330 Thousand (Tsd.) €, or 26% relative to the unidirectional case. On the other hand, Fleet V2G yields savings of 8 Tsd. €, which represents only 0.63% cost savings compared to the unidirectional case.

The transition to bidirectional operation does not result in a noticeable increase in electricity consumption, as seen in Table 2. Similarly, the overall battery degradation costs remain unchanged. While there is a slight increase in cycle costs brought on by a higher EV fleet utilization, it is countered by a slight reduction in calendar costs enabled by the flexibility in SOC management of bidirectional operations. Indeed,

Table 2
Yearly results of fleet cases.

		Unidirectional	Fleet V2G	Fleet V2G + FCR-D
Net profit	[Tsd. €]	−1264	−1256	−934
	[%] vs. uni		0.6%	26%
Feed-in profit	[Tsd. €]	12	25	17
	[%] vs. uni		108%	42%
FCR-D profit	[Tsd. €]	–	–	321
	[%] vs. uni			
E^{grid}	[MWh]	4496	4548	4494
	[%] vs. uni		1.2%	−0.1%
E^{grid_feedin}	[MWh]	195	221	191
	[%] vs. uni		12%	−2.1%
E^{char_pcc}	[MWh]	4221	4412	4348
	[%] vs. uni		4.5%	3%
E^{dis_pcc}	[MWh]	–	155	114
	[%] vs. uni			
Self-sufficiency	[%]	5.8%	5.7%	6.4%
	[%] vs. uni			
SOH loss	[%]	2.86	2.86	2.84
	[%] vs. uni		0%	−0.7%

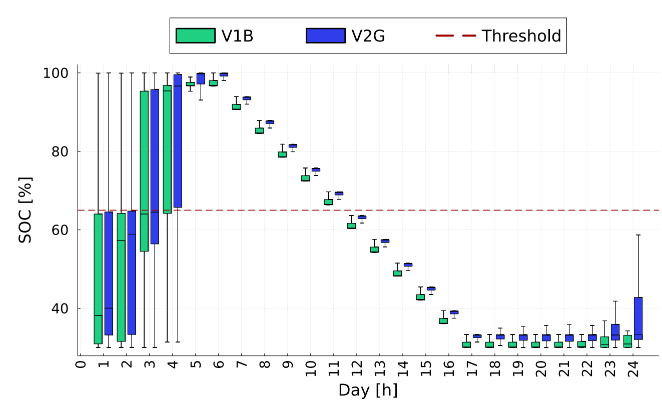

Fig. 6. State of Charge of the fleet on weekdays in winter.

the yearly SOH loss of 2.8% is the same in all cases. To explain this, Fig. 6 compares the SOC operation for weekdays in winter between V2G plus FCR-D and the unidirectional baseline.

The SOC exceeds the maximum SOC threshold and even rises to near 100% for both operations. V2G plus FCR-D seems to keep a slightly higher SOC at some hours of the day compared to the unidirectional operation, but the SOC is still kept in the same side of the threshold. Capacity fade increases only when the threshold is trespassed. Rather than

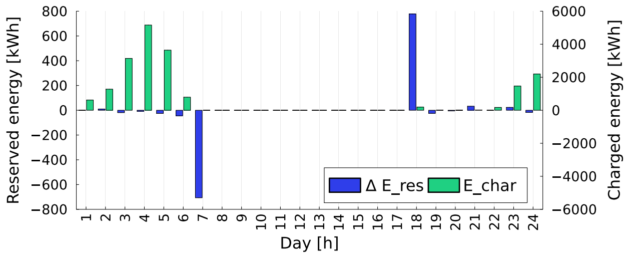

(a) Average charged and reserved energy

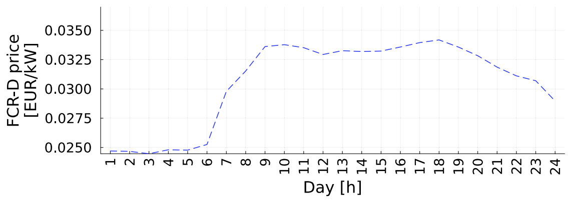

(b) Average FCR-D upregulation price

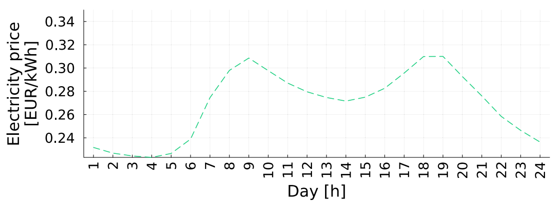

(c) Average electricity price

Fig. 7. Average FCR-D up provision on weekdays in winter.

the performance of the bidirectional service, the increased degradation is due to the high driving demand of the EV fleet. The optimization schedules charging towards the end of the period at the depot, close to 6 am, where high SOC levels happen for both operations. This way it avoids that the EVs maintain a high SOC for a longer time and thus avoids increased calendar degradation. In comparison, summer's SOC is lower, around 70%, due to lower driving demand. Still, the threshold is surpassed the same number of hours in a day as in winter. On weekends, when there is no driving demand, the SOC is kept below the threshold. Thus, low electricity prices on weekends do not outweigh additional calendar degradation costs.

After 5 pm the fleet is available at the depot to perform a bidirectional service but the SOC is near the minimum limit at 30%. In the case of Fleet V2G, if the fleet would charge after returning to the depot, the charging would occur during the peak price hours. Consequently, the EV fleet cannot satisfy building demand during these hours. Therefore, PA is rarely performed and thus self-sufficiency is low, similar to the unidirectional case. Likewise, the spot prices are not high enough during the available time slots to encourage grid feed-in. E^{grid_feedin} only differs from the unidirectional case by only 12%, still feed-in profit doubles. Bidirectional operation enables grid feed-in at higher prices, which before was limited by the occurrence of PV production. In fact, most of the PV production occurs during midday and it cannot be used by the EV fleet during working days. Because of the schedule of the EVs, their capacity, driving demand and the pricing of Fleet V2G, there is no opportunity to perform the service cost effectively.

In contrast, after the driving demand in V2G plus FCR-D there are small charging sessions occurring at 6 pm on weekdays to store energy, E^{res} and offer FCR-D up reserve with it, as illustrated in Fig. 7. E^{res} represents on average 1.3% and up until 6% of the total capacity of the fleet. As seen, E^{res} is kept until 6 am when it is taken back. According to Fig. 7, FCR-D up regulation price is generally lower than the electricity price. The short charging session at 6 pm is close to the daily peak, where FCR-D up price is around 0.034 €/kW and the electricity price around 0.29 €/kWh. However, the service is still beneficial since SOC can be kept for several hours because only a small amount of energy is ever discharged. Thus, the offered reserve P^{res} can span for consecutive hours. Seen for the full year the sum of the offered reserves amounts to 8,917 MW, two thirds of the volume allowed to offer, only constrained by the volume that can be attained by bidding in the market and the availability of the EVs.

The investment required for V2G plus FCR-D is the price change of the bidirectional chargers with respect to unidirectional. There is no publicly known information for bidirectional chargers with a power output of 100 kW. The unidirectional charger from ABB has a price of 63,750 € [63]. Adding the price difference per kW between the bidirectional and unidirectional chargers from openWB or Wallbox, respectively, the price for the bidirectional model would range between 74,062 € and 120,000 €. Then, the simple payback period of V2G plus FCR-D is 3 to 17 years, including the yearly subscriptions for availability and own producers.

Notably, the FCR-D profit demonstrates its capacity to offset the increase in all other incurred costs when an EV fleet transitions from unidirectional to bidirectional operation. V2G operation does not entail a big change in the charging and discharging patterns of an EV fleet, as the additional energy stored is low. Furthermore, V2G operation offering the FCR-D up-regulating service is suitable for the high levels of SOC and the schedule imposed by the driving demand of the EV fleet. Regardless of the difference between electricity price and FCR-D regulating price, V2G plus FCR-D proves to be beneficial as long as it can be offered in consecutive hours.

5.3. Discussion

Drawing from the results, this study delineates the economic viability of bidirectional charging while ensuring appropriate battery lifetime management across various business models. The main insights are summarized here as they may be generalized to apply as a broader reference for V2G deployment.

The cost savings indicate that bidirectional operation yields promising benefits to RUs. It is important to note that V2H and V2G perform similarly because they focus on satisfying household demand rather than feeding-in electricity into the grid, which is rarely profitable; only 2.5% of the days in the modeled year the spot price difference is high enough to exceed all arising costs. In general, the EV charges right before it is needed and during a price decline. Cost savings happen even at the lower end of the user's flexibility range because the highest electricity prices often coincide with the EV being available at home. Although battery degradation increases slightly, the model deemed it beneficial to cycle the battery for bidirectional purposes, provided it operates optimally within the SOC threshold. The service is also offered despite low efficiencies in the charging process which are irrelevant to the charging decisions.

For EV fleets, the usage patterns of the EV fleet greatly influence the feasibility of the service. For instance, although the FCR-D price is lower than the peak demand charging price, it is profitable to offer reserves for consecutive hours, allowed by the fleet's rigid schedule. Conversely, for Fleet V2G, although bidirectional operation enabled grid feed-in at higher prices, the spot price is not high enough during the available time slots to encourage its provision. Furthermore, PV support is minimal for both services as it did not align with the fleet's schedule. Regarding calendar degradation, SOH loss is similar between bidirectional and unidirectional operations. Calendar degradation is the leading cause. It is inherent to the high driving demand of the fleet rather than the performance of the bidirectional service. Hence, the optimization schedules the charging session just before driving begins to avoid higher calendar degradation by maintaining a high SOC only for short periods.

Table A.3
List of sets, variables, parameters, and scalars.

	Value	Unit	Description	Source
Sets				
t	$\in T$	h	Time steps of the optimization	
u	$\in U$	–	Users regarded in the optimization	
d	$\in D$	–	Used for implementing rolling horizon	
s	$\in S$	–	Days in summer	
w	$\in W$	–	Days in winter	
p	$\in P$	–	Power steps in charging or discharging mode	
v	$\in V$	–	Vehicles in the regarded EV fleet	
Decision variables				
$E^{grid}_{t,u}$	$\in \mathbb{R}^+_0$	kWh	Energy drawn from the grid	
$E^{dis}_{t,u}$	$\in \mathbb{R}^+_0$	kWh	Energy discharged from EV, seen from EV side	
$E^{char}_{t,u}$	$\in \mathbb{R}^+_0$	kWh	Energy charged to EV, seen from EV side	
$E^{dis\_pcc}_{t,u}$	$\in \mathbb{R}^+_0$	kWh	Energy discharged from EV, seen from grid side	
$E^{char\_pcc}_{t,u}$	$\in \mathbb{R}^+_0$	kWh	Energy charged to EV, seen from grid side	
$\delta^{cal}_{d,t,u}$	$\in \mathbb{R}^+_0$	$\frac{\%^{SOH}}{h}$	Calendar capacity loss	
$SOC_{d,t,u}$	$\in \mathbb{R}^+_0$	kWh	Energy stored in EV	
$y_{d,t,u}$	$\in \{0,1\}$	–	Implies going beyond the operating threshold of SOC	
$\rho^{char}_{t,u}$	$\in \{0,1\}$	–	Ensures the EV can only be charged within an hour	
$\rho^{dis}_{t,u}$	$\in \{0,1\}$	–	Ensures the EV can only be discharged within an hour	
$\beta^{char}_{t,p,u}$	$\in \mathbb{Z}^+_0$	–	Number of charging windows in an hour for charging	
$\beta^{dis}_{t,p,u}$	$\in \mathbb{Z}^+_0$	–	Number of charging windows in an hour for discharging	
$E^{feedin}_{t,u}$	$\in \mathbb{R}^+_0$	kWh	Energy fed into the grid by the household	
P^{res}_{t}	$\in \mathbb{R}^+_0$	kW	Power for FCR-D up reserve	
E^{res}_{t}	$\in \mathbb{R}^+_0$	kWh	Energy for FCR-D up reserve	
$res^{up}_{t,p,v}$	$\in \{0,1\}$	–	Power step for FCR-D up reserve	
Parameters				
P^{char}_{p}	–	kW	Maximum power of each charging power step	[46]
P^{dis}_{p}	–	kW	Maximum power of each discharging power step	[46]
η^{char}_{p}	–	–	Efficiency of each charging power step	[46]
η^{dis}_{p}	–	–	Efficiency of each discharging power step	[46]
$\gamma_{d,t}$	–	kWh	Household demand	[52]
$\theta_{d,t,u}$	–	–	Binary indicating if EV is available (1 = available, 0 = unavailable)	own asm.
$\kappa_{d,t,u}$	–	kWh/h	Driving consumption of EV	[42,44,45]
$\pi^{el}_{d,t}$	–	€/kWh	Electricity price for household consumers	[43,49,64]
$\pi^{spot}_{d,t}$	–	€/kWh	Day ahead spot price for the bidding zone DK2	[49]
$PV_{d,t}$	–	kWh	Energy generated by PV panels at EV fleet depot	[53,54]
$\pi^{FCR-D}_{d,t}$	–	€/kW	Price for reserved FCR-D upregulation capacity	[56]
$vol^{FCR-D}_{d,t}$	–	kW	Total volume of FCR-D up purchased	[56]
Scalar				
c	59/300	kWh	Capacity of the EV/fleet vehicle	[42]
SOC^{min}	30%	kWh	Minimum SOC for EV battery	own asm.
SOC^{max}	65%	kWh	SOC threshold for higher calendar degradation of EV battery	[37]
ω	6	–	Number of charging windows in an hour	own asm.
$\delta^{cal}_{ba,s}$	1.14E−04	$\frac{\%^{SOH}}{h}$	Base calendar capacity loss per hour at 20 °C	[38]
$\delta^{cal}_{ad,s}$	3.26E−05	$\frac{\%^{SOH}}{h}$	Additional calendar capacity loss per hour for high SOC at 20 °C	[38]
$\delta^{cal}_{ba,w}$	8.97E−05	$\frac{\%^{SOH}}{h}$	Base calendar capacity loss per hour at 10 °C	[38]
$\delta^{cal}_{ad,w}$	3.26E−05	$\frac{\%^{SOH}}{h}$	Additional calendar capacity loss per hour for high SOC at 10 °C	[38]
α^{cal}	354	$€/\%^{SOH}$	Battery degradation cost per percent of SOH	own asm.
α^{cyc}	1.062	$€/cycle$	Battery degradation cost per cycle	own asm.
τ^{TSO}	0.0616	€ct./kWh	Feed-in and balance tariffs imposed on producing electricity, set by TSO Energinet	[64]

(*continued on next page*)

Table A.3 (*continued*).

	Value	Unit	Description	Source
τ^{DSO}	0.0751 / 0.0429	€ct./kWh	Feed-in tariff imposed on producing electricity category C/A-low, set by DSO Cerius	[43]
τ^{PES}	0.536	€ct./kWh	Tariff imposed on handling electricity feed-in by PES Nettøpower	[50]
χ	5	%	Maximum market share EV fleet is allowed to cover	own asm.

6. Conclusion

V2X services can support the grid integration of EVs to achieve carbon neutrality in transportation, as well as broader system benefits. In this study, the feasibility of business models for degradation-aware bidirectional charging is examined. V2H and Residential V2G are selected for RUs, whereas Fleet V2G and Fleet V2G plus FCR-D for larger EV fleets. These services are technically and commercially ready for application in Eastern Denmark. The business models developed for each service outline their objectives, agents, and assets. Each model provides a framework for simulating the V2X service through a mathematical optimization of one year of operation. The charge and discharge decisions are optimized with the goal of cost minimization while ensuring appropriate battery lifetime management and incorporating supporting RES at the charging location for fleets.

For the RU application, V2H and V2G yield yearly cost savings of 174 € and 179 €. V2H is deemed more feasible for RUs and is expected to allow payback within 5 to 6.6 years. Battery degradation increases only slightly, due to cycle degradation. For EV fleets, V2G plus FCR-D provided cost savings of 330 Tsd. €, a 26% reduction relative to a unidirectional case, and a payback period of 3 years, in the best-case scenario. Conversely, Fleet V2G did not result in significant cost savings. The usage patterns of the EV fleet greatly influence the feasibility of the service. The yearly SOH loss was 2.86% for both bidirectional operations, similar to the one in the unidirectional case. Calendar degradation is the leading cause.

However, the outcomes of the optimization models must be regarded with certain limitations in mind. The V2G plus FCR-D model did not account for aggregator costs due to undisclosed fees. Besides, optimal bidding, assumed by using recorded market data, allowed selling maximum capacity at the highest possible price. Here, the use of stochastic or robust optimization may account for uncertainty in prices and volumes of FCR-D. Arguably, the unidirectional case could offer up reserve by interrupting charging sessions, which was not considered. Decreasing the minimum SOC could alleviate high levels for fleet vehicles that interfered with V2X service provision. It should also be noted that the benefits of V2G extend beyond those of EV users. As reviewed, V2G operation brings benefits to the system and its stakeholders. Incentives that distribute these benefits more equitably and encourage V2G operation should be investigated further. Future research could explore as well different usage patterns for RUs or fleets, different battery capacities or other ranges of flexibility leveraged by the charging power. Other services could be investigated, like offering FCR-D down reserves or both services in parallel.

CRediT authorship contribution statement

David Menchaca Santos: Writing – review & editing, Writing – original draft, Visualization, Software, Methodology, Investigation, Formal analysis, Conceptualization. **Pauline Thüne:** Writing – review & editing, Writing – original draft, Visualization, Software, Methodology, Investigation, Formal analysis, Conceptualization. **Jan Martin Zepter:** Writing – review & editing, Supervision, Methodology, Conceptualization. **Mattia Marinelli:** Writing – review & editing, Supervision, Funding acquisition, Conceptualization.

Declaration of competing interest

The authors declare that they have no known competing financial interests or personal relationships that could have appeared to influence the work reported in this paper.

Acknowledgments

This work has been financially supported by the European Union's Horizon Europe research and innovation programme through the EV4EU project (Grant Agreement No. 101056765). The authors would like to thank Anna Malkova and Steffen Nederby Høj for their valuable comments as co-supervisors for the underlying master's thesis. This work was furthermore supported by a fellowship of the German Academic Exchange Service (DAAD).

Appendix. Nomenclature of the modeling variables

See Table A.3.

Data availability

Data will be made available on request.

References

[1] European Environment Agency. EEA greenhouse gases. 2022, URL https://www.eea.europa.eu/data-and-maps/data/data-viewers/greenhouse-gases-viewer. [Online; Accessed 19 July 2024].

[2] European Alternative Fuels Observatory. Electric vehicle model statistics. 2023, URL https://alternative-fuels-observatory.ec.europa.eu/policymakers-and-public-authorities/electric-vehicle-model-statistics. [Online; Accessed 19 July 2024].

[3] International Energy Agency. Global EV Outlook 2024. 2024, URL https://www.iea.org/reports/global-ev-outlook-2024. [Online; Accessed 19 July 2024].

[4] International Energy Agency. Tracking clean energy progress 2023. Tech. rep., 2023, URL https://www.iea.org/reports/tracking-clean-energy-progress-2023.

[5] Engelhardt J, Zepter JM, Gabderakhmanova T, Marinelli M. Energy management of a multi-battery system for renewable-based high power EV charging. ETransportation 2022;14:100198. http://dx.doi.org/10.1016/j.etran.2022.100198.

[6] Montes T, Pinsach Batet F, Igualada L, Eichman J. Degradation-conscious charge management: Comparison of different techniques to include battery degradation in Electric Vehicle Charging Optimization. J Energy Storage 2024;88:111560. http://dx.doi.org/10.1016/j.est.2024.111560.

[7] Khezri R, Steen D, Tuan LA. A review on implementation of vehicle to everything (V2X): Benefits, barriers and measures. In: IEEE PES innovative smart grid technologies (ISGT) Europe. 2022, p. 1–6.

[8] Thompson AW, Perez Y. Vehicle-to-everything (V2X) energy services, value streams, and regulatory policy implications. Energy Policy 2020;137:111136. http://dx.doi.org/10.1016/j.enpol.2019.111136.

[9] Rehman MA. A comprehensive overview of vehicle to everything (V2X) technology for sustainable EV adoption. J Energy Storage 2023;74:109304. http://dx.doi.org/10.1016/j.est.2023.109304.

[10] Pearre NS, Ribberink H. Review of research on V2X technologies, strategies, and operations. Renew Sustain Energy Rev 2019;105:61–70. http://dx.doi.org/10.1016/j.rser.2019.01.047.

[11] Ledro M, Calearo L, Zepter JM, Gabderakhmanova T, Marinelli M. Influence of realistic EV fleet response with power and energy controllers in an EV-wind virtual power plant. Sustain Energy Grids Netw 2022;31:100704. http://dx.doi.org/10.1016/j.segan.2022.100704.

[12] Gough R, Dickerson C, Rowley P, Walsh C. Vehicle-to-grid feasibility: A techno-economic analysis of EV-based energy storage. Appl Energy 2017;192:12–23. http://dx.doi.org/10.1016/j.apenergy.2017.01.102.

[13] Lotfi M, Almeida T, Javadi MS, Osório GJ, Monteiro C, Catalão JP. Coordinating energy management systems in smart cities with electric vehicles. Appl Energy 2022;307:118241. http://dx.doi.org/10.1016/j.apenergy.2021.118241.
[14] Wu W, Lin B. Benefits of electric vehicles integrating into power grid. Energy 2021;224:120108. http://dx.doi.org/10.1016/j.energy.2021.120108.
[15] Ahmadian A, Sedghi M, Mohammadi-ivatloo B, Elkamel A, Aliakbar Golkar M, Fowler M. Cost-benefit analysis of V2G implementation in distribution networks considering PEVs battery degradation. IEEE Trans Sustain Energy 2018;9(2):961–70. http://dx.doi.org/10.1109/TSTE.2017.2768437.
[16] Geng J, Bai B, Hao H, Sun X, Liu M, Liu Z, Zhao F. Assessment of vehicle-side costs and profits of providing vehicle-to-grid services. ETransportation 2024;19:100303. http://dx.doi.org/10.1016/j.etran.2023.100303.
[17] Leippi A, Fleschutz M, Davis K, Klingler A-L, Murphy MD. Optimizing electric vehicle fleet integration in industrial demand response: Maximizing vehicle-to-grid benefits while compensating vehicle owners for battery degradation. Appl Energy 2024;374:123995. http://dx.doi.org/10.1016/j.apenergy.2024.123995.
[18] Jaworski J, Zheng N, Preindl M, Xu B. Vehicle-to-grid fleet service provision considering nonlinear battery behaviors. IEEE Trans Transp Electrif 2024;10(2):2945–55. http://dx.doi.org/10.1109/TTE.2023.3305235.
[19] Brinkel N, Zijlstra M, van Bezu R, van Twuijver T, Lampropoulos I, van Sark W. A comparative analysis of charging strategies for battery electric buses in wholesale electricity and ancillary services markets. Transp Res E Logist Transp Rev 2023;172:103085. http://dx.doi.org/10.1016/j.tre.2023.103085.
[20] Manzolli JA, Trovão JPF, Henggeler Antunes C. Electric bus coordinated charging strategy considering V2G and battery degradation. Energy 2022;254:124252. http://dx.doi.org/10.1016/j.energy.2022.124252.
[21] Gschwendtner C, Sinsel SR, Stephan A. Vehicle-to-X (V2X) implementation: An overview of predominate trial configurations and technical, social and regulatory challenges. Renew Sustain Energy Rev 2021;145:110977. http://dx.doi.org/10.1016/j.rser.2021.110977.
[22] Marinelli M, Calearo L, Ried S, Pfab X, Diaz Cabrera JC, Spalthoff C, et al. Electric vehicles demonstration projects - An overview across Europe. In: 2020 55th international universities power engineering conference. 2020, p. 1–6. http://dx.doi.org/10.1109/UPEC49904.2020.9209862.
[23] Sevdari K, Calearo L, Andersen PB, Marinelli M. Ancillary services and electric vehicles: An overview from charging clusters and chargers technology perspectives. Renew Sustain Energy Rev 2022;167:112666. http://dx.doi.org/10.1016/j.rser.2022.112666.
[24] SSE. Bus2Grid. 2023, URL https://www.sseenergysolutions.co.uk/distributed-energy-infrastructure/our-solutions/bus2grid. [Online; Accessed 28 September 2023].
[25] V2G Hub. Bus2Grid. 2023, URL https://www.v2g-hub.com/projects/bus2grid. [Online; Accessed 28 September 2023].
[26] Moor A. V2G electric school bus commercialization project. 2021, URL https://www.energy.gov/sites/default/files/2021-06/elt095_moore_2021_o_5-14_416pm_LR_TM.pdf. [Online; Accessed 28 September 2023].
[27] V2Go! – Demonstrating the value of vehicle-to-grid charging for fleets. 2019, URL https://www.v2go.org. [Online; Accessed 28 September 2023].
[28] V2G Hub. V2GO. 2024, URL https://www.v2g-hub.com/projects/v2go. [Online; Accessed 28 September 2023].
[29] Zheng Y, Shao Z, Shang Y, Jian L. Modeling the temporal and economic feasibility of electric vehicles providing vehicle-to-grid services in the electricity market under different charging scenarios. J Energy Storage 2023;68:107579. http://dx.doi.org/10.1016/j.est.2023.107579.
[30] Recalde Melo DF, Trippe A, Gooi HB, Massier T. Robust electric vehicle aggregation for ancillary service provision considering battery aging. IEEE Trans Smart Grid 2018;9(3):1728–38. http://dx.doi.org/10.1109/TSG.2016.2598851.
[31] Lyu R, Guo H, Zheng K, Sun M, Chen Q. Co-optimizing bidding and power allocation of an EV aggregator providing real-time frequency regulation service. IEEE Trans Smart Grid 2023;14(6):4594–606. http://dx.doi.org/10.1109/TSG.2023.3252664.
[32] Khezri R, Steen D, Wikner E, Tuan LA. Optimal V2G scheduling of an EV with calendar and cycle aging of battery: An MILP approach. IEEE Trans Transp Electrif 2024;1. http://dx.doi.org/10.1109/TTE.2024.3384293.
[33] Wikner E, Thiringer T. Extending battery lifetime by avoiding high SOC. Appl Sci 2018;8(10). http://dx.doi.org/10.3390/app8101825.
[34] Aziz M, Huda M. Utilization of electric vehicles for frequency regulation in Danish electrical grid. Energy Procedia 2019;158:3020–5. http://dx.doi.org/10.1016/j.egypro.2019.01.977.
[35] Bach Andersen P, Hashemi Toghroljerdi S, Meier Sørensen T, Christensen BE, Morell Lodberg Høj JC, Zecchino A. The Parker Project: Final Report. 2019, URL https://parker-project.com/wp-content/uploads/2019/03/Parker_Final-report_v1.1_2019.pdf. [Online; Accessed 25 September 2023].
[36] Thompson AW. Economic implications of lithium ion battery degradation for Vehicle-to-Grid (V2X) services. J Power Sources 2018;396:691–709. http://dx.doi.org/10.1016/j.jpowsour.2018.06.053.
[37] Keil P. Calendar aging of lithium-ion batteries. J Electrochem Soc 2016;163. http://dx.doi.org/10.1149/2.0411609jes.
[38] Marinelli M, Calearo L, Engelhardt J. A simplified electric vehicle battery degradation model validated with the nissan LEAF e-plus 62-kWh. In: proceedings of 6th international electric vehicle technology conference. 2023.
[39] Thingvad A, Ziras C, Ray GL, Engelhardt J, Mosbæk RR, Marinelli M. Economic value of multi-market bidding in nordic frequency markets. In: 2022 international conference on renewable energies and smart technologies, vol. I. 2022, p. 1–5. http://dx.doi.org/10.1109/REST54687.2022.10023471.
[40] JuMP. Jump - home. 2024, URL https://alternative-fuels-observatory.ec.europa.eu/transport-mode/road/denmark/incentives-legislations.
[41] Bloom N, Han R, Liang J. How hybrid working from home works out. Working paper series no. 30292, National Bureau of Economic Research; 2022, http://dx.doi.org/10.3386/w30292, URL http://www.nber.org/papers/w30292.
[42] Nissan. Nissan LEAF & LEAF e+: Prisliste, Udstyr & Specifikationer. Nissan; 2023, URL https://www.nissan.dk/content/dam/Nissan/dk/brochures/cpls/LEAF_Kundeprisliste_MY22.pdf.
[43] Cerius. Tariffer og netabonnement - Cerius. 2023, https://cerius.dk/priser-og-tariffer/tariffer-og-netabonnement/?_gl=1*n1e3fy*_up*MQ..*_ga*MTgwODMzMjkwLjE2OTg3NDQzMjc.*_ga_K31DDG1SNZ*MTY5ODc0NDMyNi4xLjEuMTY5ODc0NDM1Ni4wLjAuMA. [Online; Accessed 31 October 2023].
[44] Dost P, Spichartz P, Sourkounis C. Temperature influence on state-of-the-art electric vehicles' consumption based on fleet measurements. In: 2015 international conference on electrical systems for aircraft, railway, ship propulsion and road vehicles. ESARS, 2015, p. 1–6. http://dx.doi.org/10.1109/ESARS.2015.7101504.
[45] StatBank Denmark. 2023, URL https://www.statbank.dk/statbank5a/default.asp?w=1440. [Online; Accessed 20 November 2023].
[46] Fronius. Fronius Symo 6.0-3-M. 2023, URL https://www.fronius.com/en-gb/uk/solar-energy/installers-partners/technical-data/all-products/inverters/fronius-symo/fronius-symo-6-0-3-m. [Online; Accessed 20 November 2023].
[47] Thingvad A, Calearo L, Andersen PB, Marinelli M. Empirical capacity measurements of electric vehicles subject to battery degradation from V2G service. IEEE Trans Veh Technol 2021;70:7547–57. http://dx.doi.org/10.1109/TVT.2021.3093161.
[48] Hørby C, Lomholt L. Vehicle-to-grid services for prosumers in Denmark. 2023, URL https://orbit.dtu.dk/en/activities/vehicle-to-grid-services-for-prosumers-in-denmark. [Online; Accessed 8 December 2023].
[49] Nordpool. See hourly day-ahead prices. 2023, URL https://www.nordpoolgroup.com/en/Market-data1/Dayahead/Area-Prices/DK/Hourly/?view=table. [Online; Accessed 20 November 2023].
[50] Nettø power. Sælg din strøm og bliv produktionselleverandør. 2023, URL https://www.nettopower.dk/el/saelg-din-stroem. [Online; Accessed 4 December 2023].
[51] European Alternative Fuels Observatory. Incentives and legislation. 2024, URL https://alternative-fuels-observatory.ec.europa.eu/transport-mode/road/denmark/incentives-legislations.
[52] Radius. Elforbrug - Radius. 2022, URL https://radiuselnet.dk/om-elnettet/dyk-ned-i-elforbruget/?_gl=1*1kn1rkx*_up*MQ..*_ga*MTMxNDgyMTU2Ni4xNjk2ODUwMDU1*_ga_TRQXB95J5R*MTY5Njg1MDA1NC4xLjEuMTY5Njg1MDA4Mi4wLjAuMA. [Online; Accessed 20 November 2023].
[53] EV4EU. Home - EV4EU. 2023, URL https://ev4eu.eu. [Online; Accessed 11 October 2023].
[54] Home - Insulae h2020. 2021, URL http://insulae-h2020.eu. [Online; Accessed 28 September 2023].
[55] Zepter JM, Engelhardt J, Ledro M, Gabderakhmanova T, Marinelli M. Experimental assessment of active power control of distributed generation units. Sustain Energy Technol Assess 2023;60:103500. http://dx.doi.org/10.1016/j.seta.2023.103500.
[56] Energinet. FCR N and D, frequency containment reserves, DK2. 2023, URL https://www.energidataservice.dk/tso-electricity/FcrNdDK2.
[57] Energinet. Outlook for ancillary services 2023–2040. 2024, URL https://en.energinet.dk/electricity/ancillary-services/ancillary-services-in-the-future/.
[58] Zepter JM, Engelhardt J, Gabderakhmanova T, Marinelli M. Re-thinking the definition of self-sufficiency in systems with energy storage. In: Proceedings of 2022 international conference on smart energy systems and technologies. SEST, IEEE; 2022, http://dx.doi.org/10.1109/SEST53650.2022.9898436.
[59] openWB. openWB Pro. 2024, https://openwb.de/shop/?product=openwb-pro. [Online; Accessed 6 October 2023].
[60] openWB series2 standard – openWB. 2024, URL https://openwb.de/shop/?product=openwb-series-2-standard-2. [Online; Accessed 12 January 2024].
[61] E-mobileo. Bidirektionale Wallboxen – Modelle, Preise und Empfehlungen. 2022, URL https://www.e-mobileo.de/bidirektionale-wallboxen-und-ladestationen. [Online; Accessed 6 October 2024].
[62] Wallbox pulsar plus electric vehicle charger. Amazon.com; 2024, URL https://www.amazon.de/Wallbox-Elektrofahrzeuge-Einstellbarer-Bluetooth-Verbindung-OCPP-kompatibel/dp/B095B29DFH.
[63] ABB Terra DC 124 - fast charging station - #1 choice in Europe. 2023, URL https://chargingshop.eu/de/product/abb-terra-124-dc-model-fast-charging-station. [Online; Accessed 24 January 2024].
[64] Energinet. Aktuelle tariffer. 2023, URL https://energinet.dk/el/elmarkedet/tariffer/aktuelle-tariffer. [Online; Accessed 20 November 2023].